AEM
Journals.ASM.org

Inactivation of *Escherichia coli* Cells in Aqueous Solution by Atmospheric-Pressure N_2, He, Air, and O_2 Microplasmas

Renwu Zhou,[a] Xianhui Zhang,[a] Zhenhua Bi,[b] Zichao Zong,[b] Jinhai Niu,[b] Ying Song,[b] Dongping Liu,[a,b] Size Yang[a]

Fujian Provincial Key Laboratory for Plasma and Magnetic Resonance, Institute of Electromagnetics and Acoustics, Department of Electronic Science, School of Physics and Mechanical and Electrical Engineering, Xiamen University, Xiamen, People's Republic of China[a]; Liaoning Key Laboratory of Optoelectronic Films and Materials, School of Physics and Materials Engineering, Dalian Nationalities University, Dalian, People's Republic of China[b]

Atmospheric-pressure N_2, He, air, and O_2 microplasma arrays have been used to inactivate *Escherichia coli* cells suspended in aqueous solution. Measurements show that the efficiency of inactivation of *E. coli* cells is strongly dependent on the feed gases used, the plasma treatment time, and the discharge power. Compared to atmospheric-pressure N_2 and He microplasma arrays, air and O_2 microplasma arrays may be utilized to more efficiently kill *E. coli* cells in aqueous solution. The efficiencies of inactivation of *E. coli* cells in water can be well described by using the chemical reaction rate model, where reactive oxygen species play a crucial role in the inactivation process. Analysis indicates that plasma-generated reactive species can react with *E. coli* cells in water by direct or indirect interactions.

Plasma, called the fourth fundamental state of matter, in addition to solids, liquids, and gases, consists of equal numbers of positive ions and negative electrons (negative ions in some cases) and other reactive species, generally resulting from the ionization of neutral gases. Due to the reactive species in plasma, gas-based reactive plasmas are thought to be effective in killing various microorganisms (1–3). Therefore, recently, the inactivation of microorganisms in water by atmospheric-pressure cold plasmas (APCP) has attracted great attention for biomedical and environmental applications due to their lethal effects on bacteria and fungi (4–8), since APCP include many reactive species similar to those in the conventional methods of microorganism inactivation, such as ozone generation (9), UV irradiation (10), chemical agents (11), electrical fields (12, 13), and microwave irradiation (14).

The chemical reaction rates of these plasma-activated species may be improved greatly when atmospheric-pressure nonequilibrium plasmas are generated in water (4–7, 15). These short-lived species can be formed in the vicinity of microorganisms and efficiently kill microorganisms in water. Usually, it is relatively hard to generate stable atmospheric-pressure plasmas in water. Among various plasma sources (4, 5, 7), atmospheric-pressure arc discharge has frequently been used for killing microorganisms in water. Compared to other sources, the strong arc discharges are less influenced by the aqueous environment while obviously leading to an increase in the water temperature with high energy consumption. This arc discharge can also cause serious damage to heat-sensitive materials, and the volume of treated aqueous solution is limited, since the arc plasma is usually controllable only in a small processing space.

Previously (16), we designed an atmospheric-pressure air microplasma array to inactivate *Pseudomonas fluorescens* cells in aqueous media. The microplasma produced by hollow-fiber-based microplasma jets is stable and extremely efficient in killing *P. fluorescens* cells in aqueous media. This design demonstrates potential application for large-volume plasma inactivation of bacterial cells in water. In this study, we report on the influence of He, air, N_2, and O_2 feed gases and the discharge voltage on the efficiency of inactivation of *Escherichia coli* cells in water. The inactivation of *E. coli* cells was evaluated via CFU counts on petri dishes. The efficiencies of inactivation of *E. coli* cells treated by the microplasma arrays were compared to that in H_2O_2 solution. To determine the discharge processes that take place within the plasma and their properties, optical emission spectroscopy (OES) was utilized to monitor optical emissions of plasmas. As it does not interfere with the plasma itself, information on the undisturbed plasma could be obtained. In OES, the spectrum of the radiation emitted by the plasma is sliced and its intensity is measured as a function of the wavelength. In addition, the discharge power of He, air, N_2, and O_2 microplasma arrays was measured as a function of the discharge voltage, and the processes of inactivation of *E. coli* cells in water by this method are discussed based on the experimental results.

MATERIALS AND METHODS

Plasma reactor and multiglow mode discharge. A schematic diagram of the microplasma array device is shown in Fig. 1 (7). The plasma device is mainly composed of microplasma jet units housed in a glass cup. In each microplasma jet unit, two hollow fibers with inner diameters of 200 μm and 1,500 μm are used to generate the microplasma inside the thicker hollow fiber. The 200-μm-thick tungsten wire, acting as a high-voltage electrode, is inserted into a 200-μm-inner-diameter fiber sealed at one end. The 200-μm-inner-diameter fiber is inserted into the 1,500-μm-inner-diameter fiber, and the separation between their ends is fixed at 3 mm. In this study, 6 by 6 microplasma jet units were uniformly distributed inside the glass cup with an inner diameter of 70 mm. The feed gases,

Received 19 April 2015 Accepted 20 May 2015
Accepted manuscript posted online 29 May 2015
Citation Zhou R, Zhang X, Bi Z, Zong Z, Niu J, Song Y, Liu D, Yang S. 2015. Inactivation of *Escherichia coli* cells in aqueous solution by atmospheric-pressure N_2, He, air, and O_2 microplasmas. Appl Environ Microbiol 81:5257–5265. doi:10.1128/AEM.01287-15.
Editor: V. Müller
Address correspondence to Dongping Liu, Dongping.liu@dlnu.edu.cn.
Copyright © 2015, American Society for Microbiology. All Rights Reserved.
doi:10.1128/AEM.01287-15

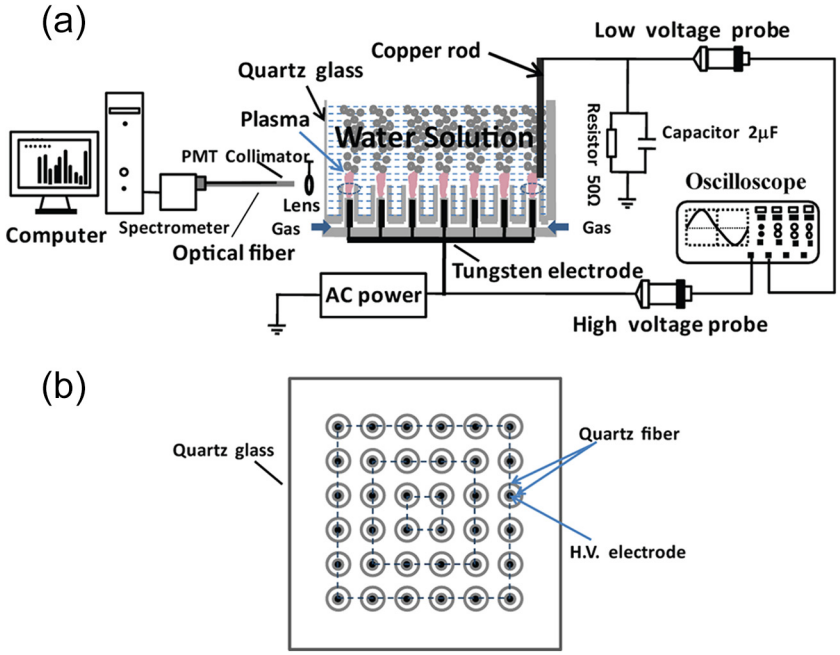

FIG 1 Schematic diagram of the experimental setup used in this study. (a) Cross-sectional view of the microplasma array device. (b) Top view of the plasma device. PMT, photomultiplier; H.V., high voltage.

such as He, N_2, air (artificial air), and O_2, were added to the 36 microplasma jet units at a flow rate of 2.0 standard liters per minute (SLM). One tungsten bar was immersed in aqueous solution, and the tungsten bar was connected to the ground. The aqueous solution containing *E. coli* cells acted as the grounded electrode. The power supply mainly consisted of a signal generator, a power amplifier, and a transformer. The signal generator is used to adjust the applied voltage and its frequency. The power supply is capable of supplying bipolar AC output with a peak voltage (V_P) of 0 to 20 kV at an AC frequency of 9.0 kHz.

Experimental procedures. (i) *E. coli* cells treated with atmospheric-pressure microplasmas. To treat *E. coli* cells with atmospheric-pressure microplasmas, a single *E. coli* colony was inoculated into approximately 200 ml LB liquid medium (tryptone, 2 g; yeast extract, 1 g; NaCl, 2 g; distilled water, 200 g; pH 7.2) and was cultivated on a shaking table with a rotation speed of 200 rpm at 28°C for 24 h. Then, 8 ml of the original solution of *E. coli* at a concentration of 10^8 CFU/ml was transferred to 800 ml sodium chloride solution (1% NaCl) for plasma inactivation. In order to avoid the effect of residual gas in solution on the inactivation efficiency, the working gas was injected into the solution before plasma inactivation. The solution, with an *E. coli* concentration of 10^6 CFU/ml, was treated with an atmospheric-pressure N_2, He, air, or O_2 microplasma array, while the untreated solution was used as the control. The plasma inactivation treatment was performed in a V_P range from 0.8 to 7.0 kV. After plasma inactivation, 1 ml of treated solution was centrifuged at a rotation speed of 3,000 rpm for 10 min. Then, the deposit at the bottom of the centrifuged solution was separated from the suspension and dissolved in 100 μl distilled water. This solution was then spread over the LB agar medium and inoculated for 24 h at 37°C.

(ii) *E. coli* cells treated with H_2O_2 solution. The hydrogen peroxide (H_2O_2) inactivation of *E. coli* cells was performed for different inactivation times. The hydrogen peroxide and *E. coli* concentrations were 5.0 to 10% and 10^7 CFU/ml, respectively. *E. coli* solution (6 μl) was transferred to 100 μl H_2O_2 solution for H_2O_2 inactivation. After a certain time, 100 ml distilled water was added to the H_2O_2 solution to slow down or stop the oxidation reaction. The solution was centrifuged with a rotation speed of 3,000 rpm for 10 min, and the deposit in the bottom of the centrifuged solution was used for inoculation of the petri dishes. The bacterial samples were inoculated on standard petri dishes 9 cm in diameter containing 15 ml LB solid medium. The static cultivation was kept at 37°C for 24 h before the bacterial counting procedure.

Analytical methods. (i) Measurement of electrical and optical characteristics. The applied voltage and discharge current were measured by using a Tektronix 2040 digital oscilloscope with a high-voltage probe and a current probe. The Lissajous figure of the microplasma array in water was obtained by measuring the charges across the capacitor (2.0 μF) in series to ground and the applied voltage across the discharge device. The Lissajous figure is used to calculate the discharge power (17). Because the optical emission spectra of an atom or molecule contain specific information about the atom or molecule, they can be used to identify the major excited reactive species generated by the N_2, He, air, or O_2 plasma in water. OES data were obtained by using a SpectraPro-750i monochromator (Acton Research Corporation) with a resolution of 0.5 nm in the wavelength range of 200 to 800 nm. One end of the fiber optics cable was used to acquire light signals through a focus lens at a distance of approximately 5 mm from the side of the quartz glass, as shown in Fig. 1a. By OES of different gaseous plasmas, we investigated the global levels of reactive oxygen species (ROS) generated by plasma in the solution.

(ii) pH values and temperatures of treated solutions. The pH values of plasma-treated solutions were measured immediately after exposure to N_2, He, air, or O_2 plasmas by using a pH meter (model Lab-850; SI Analytics Co., Mainz, Germany). The temperature of the plasma-treated solution was measured immediately after the plasma treatment using a mercury thermometer. Our measurements showed that the temperature of the plasmas-treated cultures was usually lower than 40°C.

(iii) ROS concentrations of treated solutions. The iodide oxidation-reduction ($2I^- \leftrightarrow I_2$) method was used to measure the concentration of ROS in the hydrogen peroxide solutions and plasma-treated water (18). In this study, plasma-generated ROS typically included H_2O_2, HO_2, O_3, and nitrogen oxide (NO_x) molecules and HNO_x and O and OH radicals in the gas phase. An excess of manganese(II) salt and iodide (I^-) and hydroxide (OH^-) ions were immediately added to the solution sample once the solution was treated with the atmospheric-pressure microplasma array. This manganese(II) salt was then oxidized by the ROS in solution into a

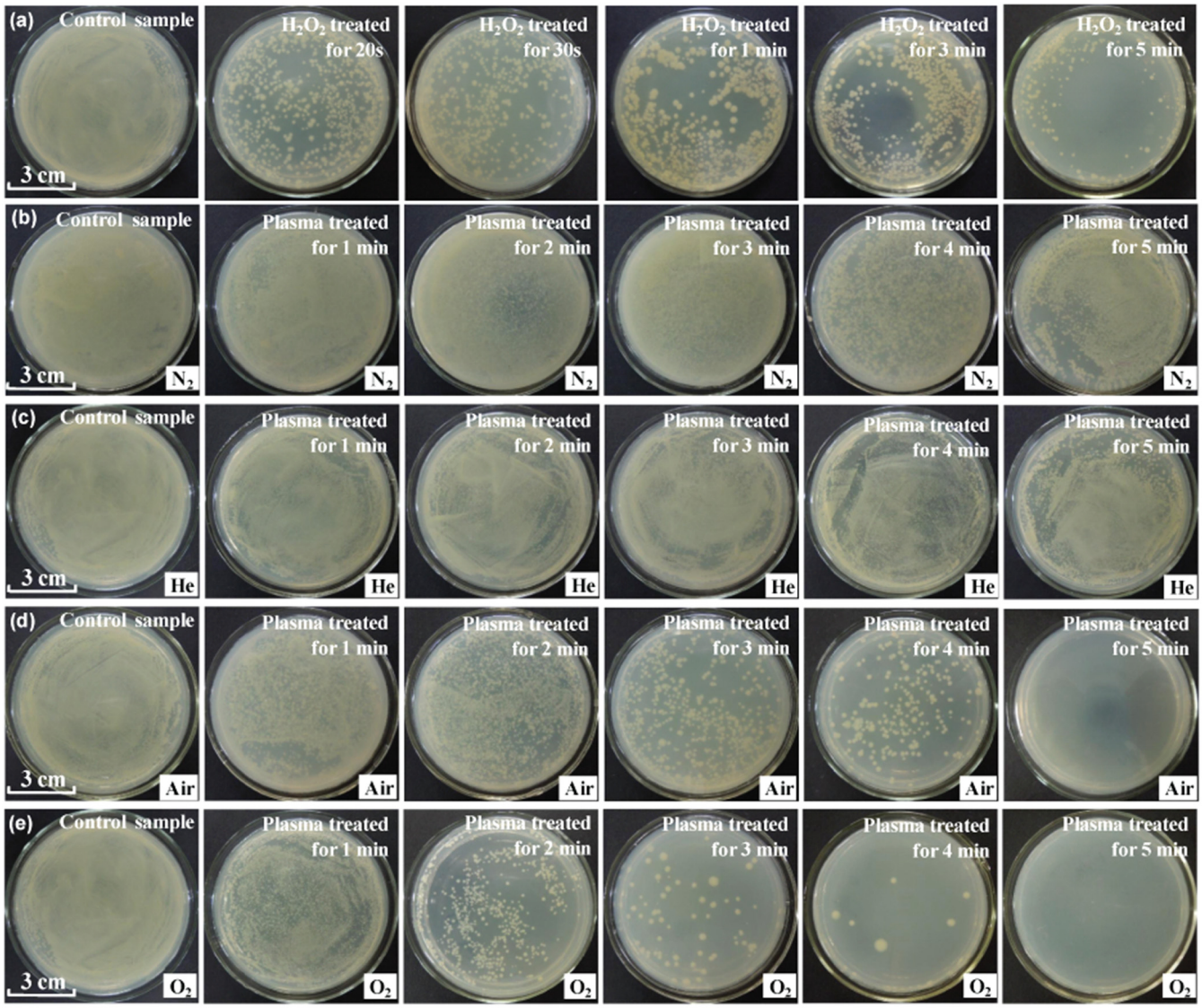

FIG 2 Photographs of samples of *E. coli* solution after treatment, spreading on agar plates, and incubation. The solution was treated with 5% hydrogen peroxide solution (row a), a N_2 microplasma array (row b), a He microplasma array (row c), an air microplasma array (row d), and an O_2 microplasma array (row e). The plasma treatments were performed at a V_P of 4.5 kV with different treatment times.

brown manganese precipitate. In the next step, strong sulfuric acid was added to acidify the solution. The brown precipitate then converted the iodide ions (I^-) to iodine. Then, thiosulfate was used with a starch indicator to titrate the iodine: $2S_2O_3^{2-}(aq) + I_2 \rightarrow S_4O_6^{2-}(aq) + 2I^-(aq)$. The amount of ROS in solution is directly proportional to the titration of iodine with a thiosulfate solution.

Statistical analysis. The experimental data, including inactivation efficiencies under different feed gases, discharge voltages, and treatment times, was statistically analyzed using one-way analysis of variance (ANOVA) and linear regression analysis. *P* values below 0.05 indicated a statistically significant difference. It should be pointed out that all the bacterial-inactivation experiments reported here were repeated four times, and the results were consistent with the experimental conditions. The inactivation of *E. coli* cells was evaluated via the CFU counts on petri dishes. For visible but not countable sample plates, a dilution method was used to count *E. coli* colony units, and then the dilution ratio was multiplied accordingly.

RESULTS

Chemical reaction rate model and inactivation efficiency. Figure 2 shows photographs of samples of *E. coli* solution after treatment, spreading on agar plates, and incubation. The solution was treated by using 5% hydrogen peroxide solution (row a), a N_2 microplasma array (row b), a He microplasma array (row c), an air microplasma array (row d), and an O_2 microplasma array (row e). The plasma treatments were performed at a V_P of 4.5 kV for different times. Clearly, the efficiency of inactivation of *E. coli* cells by H_2O_2 solution is significantly dependent on the treatment time, while the plasma inactivation efficiency depends on both the treatment time and the feed gases used. Among these inactivation methods, O_2 and air plasmas are more effective in killing *E. coli* cells in water. Figure 3a shows the $\log(C_t/C_0)$ values for 5% and 10% H_2O_2 solutions as a function of treatment time, where C_t and

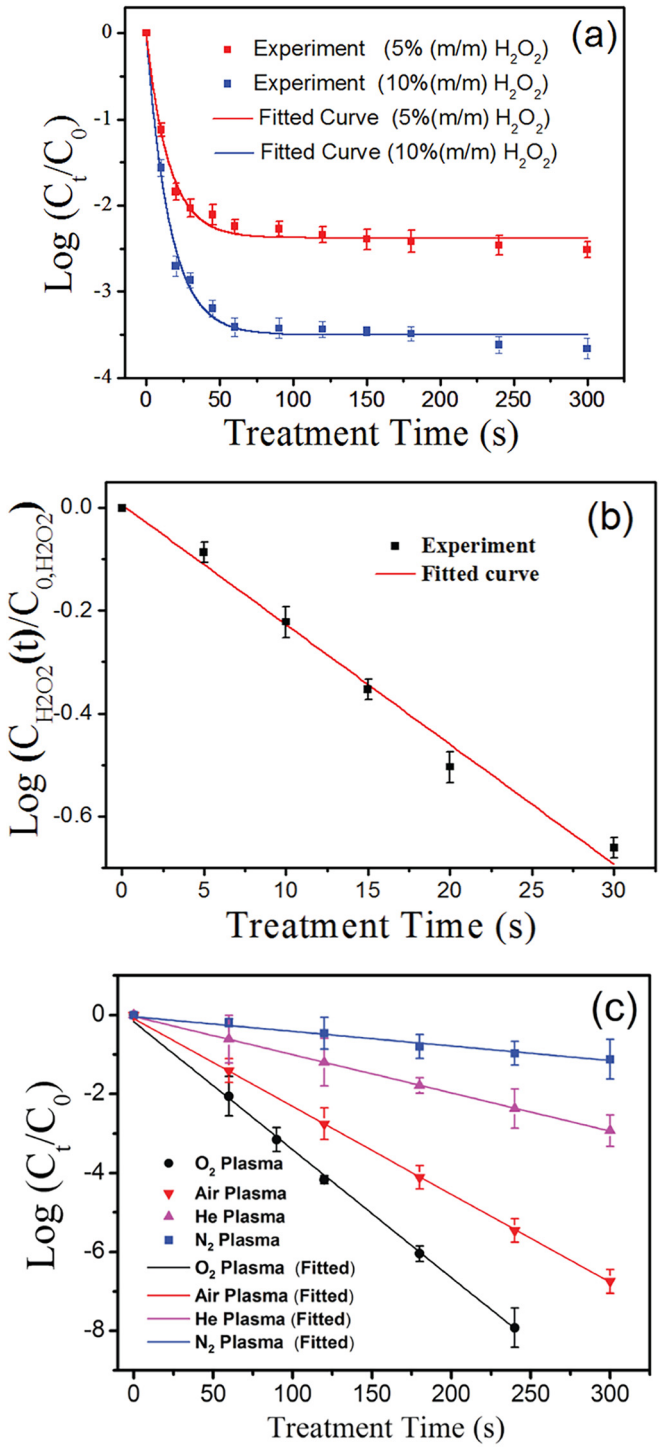

FIG 3 (a) Comparison between the $\log(C_t/C_0)$ values obtained in 5% and 10% H_2O_2 solutions within different treatment times and fitted theoretically using equation 6. m/m, mass fraction. (b) Comparison between the $\log[C_{H2O2}(t)/C_{0,H2O2}]$ values obtained in the 5% H_2O_2 solution with different treatment times and fitted theoretically using equation 3. (c) Comparison between $\log(C_t/C_0)$ values obtained under He, N_2, air, and O_2 plasma treatments and fitted theoretically using equation 9. The data points and error bars represent, respectively, the averages and standard deviations from four independent measurements.

C_0 are the concentration of *E. coli* cells alive at the treatment time (t) and the concentration of *E. coli* cells alive at time zero, respectively. When the treatment time increases from 0 to 50 s, the $\log(C_t/C_0)$ value is rapidly reduced, and then it begins to decrease slowly at a t of >50 s. The rapid decrease in the $\log(C_t/C_0)$ value suggests that *E. coli* cells are efficiently inactivated in the H_2O_2 solution at this initial stage.

The H_2O_2 molecule acting as one oxidant in the solution can react with organisms (Org), such as *E. coli* cells, as shown below (19).

$$H_2O_2 + \text{Org} \rightarrow H_2O + \text{Org(oxidized)} \quad (1)$$

By this chemical reaction, organisms are oxidized. The organisms are usually big enough to react with a large number of H_2O_2 molecules. The chemical reaction rate can be written as follows:

$$\frac{dC_{H2O2}(t)}{dt} = -k' C_{Org} C_{H2O2}(t) \quad (2)$$

where C_{Org} is the concentration of organisms, $C_{H2O2}(t)$ is the concentration of H_2O_2 at the inactivation time (t), and k' is the rate constant of the chemical reaction. The reaction calculation does not take into account the spontaneous degradation of H_2O_2 to water in solution, as well as the possible influence of iron residues from the bacterial medium. The C_{Org} value does not change significantly when the inactivation time is improved. Thus, one can obtain $C_{H2O2}(t)$ values as a function of t as follows:

$$C_{H2O2}(t) = C_{0,H2O2} \exp(-k' C_{Org} t) = C_{0,H2O2} 10^{-\beta t} \quad (3)$$

where the value of the equation $\beta = k' C_{Org} \log e$ is constant and $C_{0,H2O2}$ is the initial concentration of H_2O_2. At a certain time (t), the H_2O_2 solution containing *E. coli* cells may be immediately diluted 1,000 times to prevent or slow down the chemical reaction between H_2O_2 molecules and *E. coli* cells. Then, the iodide oxidation-reduction ($2I^- \leftrightarrow I_2$) method is utilized to measure the concentration of H_2O_2 in the solution. Figure 3b shows a comparison between the $\log[C_{H2O2}(t)/C_{0,H2O2}]$ values obtained in the 5% H_2O_2 solution within different treatment times and fitted theoretically by using equation 3. This linear fitting leads to a β of 0.023 s^{-1} and shows good consistency with the measured values. The resulting correlation coefficient is higher than 0.991.

E. coli cells alive in water can be inactivated during their interactions with H_2O_2 molecules. One *E. coli* cell is assumed to be completely inactivated after being oxidized by α H_2O_2 molecules. The chemical reaction rate can be written as follows:

$$\frac{dC_t}{dt} = -k [C_{H2O2}(t)]^{\alpha} C_t \quad (4)$$

where C_t is the *E. coli* concentration at the treatment time (t), α is the mean value for inactivating one *E. coli* cell, and k is the rate constant of the chemical reaction. Combining equations 3 and 4, one can obtain equation 5:

$$\frac{dC_t}{dt} = -k [C_{0,H2O2} \exp(-k' C_{Org} t)]^{\alpha} C_t \quad (5)$$

Solving equation 5, one can obtain equation 6:

$$\ln\left(\frac{C_t}{C_0}\right) = \frac{k C_{0,H2O2}^{\alpha}}{\alpha k' C_{Org}} (10^{-\alpha\beta t} - 1) = k_1 \left(10^{-k_2 t} - 1\right) \quad (6)$$

where the values of the equations $k_1 = k C_{0,H2O2}{}^{\alpha} / \alpha k' C_{Org}$ and $k_2 = \alpha\beta = \alpha k' C_{Org} \log e$ are constant. Figure 3a shows a compar-

ison between the $\log(C_t/C_0)$ values obtained in 5% and 10% H_2O_2 solutions within different treatment times and fitted theoretically by using equation 6. These fittings lead to a k_1 of 5.5 and a k_2 of 0.028 s^{-1} for 5% H_2O_2 solution and a k_1 of 8.1 and a k_2 of 0.027 s^{-1} for 10% H_2O_2 solution. These fittings are consistent with the experimental data (for all comparisons, $P < 0.05$ by ANOVA), indicating that the rapid decrease in the $\log(C_t/C_0)$ value can be attributed to the high H_2O_2 concentration at this initial stage. The H_2O_2 molecules in aqueous solution are completely in contact with *E. coli* cells and efficiently react with *E. coli* cells in solution. However, at increasing treatment times, the H_2O_2 concentration is greatly reduced due to the interaction with organisms. This results in a rapid decrease in the rate of change of the *E. coli* cell concentration (dC_t/dt). Therefore, the concentration of *E. coli* cells alive in the solution slowly decreases when the treatment time is improved.

The $\log(C_t/C_0)$ values were measured as a function of the He, N_2, air, or O_2 plasma treatment time, as shown in Fig. 3c. The $\log(C_t/C_0)$ value obviously decreases with increasing treatment time. The $\log(C_t/C_0)$ values are strongly dependent on the treatment time and the feed gases used. The oxidation processes of plasma-generated oxidants, such as O, OH, H_2O_2, or O_3 can play the most important role in inactivating microorganisms (2, 20, 21). These species can dissolve in the aqueous solution and then react with *E. coli* cells. A large number of microbubbles are formed close to the ends of hollow-core fibers (16). The atmospheric-pressure microplasmas are generated inside these microbubbles. The oxidants generated in the gas phase can collide with *E. coli* cells suspended in water and react directly with *E. coli* cells, resulting in the inactivation of the *E. coli* cells. If the plasma inactivation of bacterial cells is controlled by one specific oxidation reaction, the reaction processes resulting in the inactivation of *E. coli* cells can be briefly described as follows:

$$\alpha\text{ROS} + E.\ coli(\text{alive}) \rightarrow E.\ coli(\text{dead}) \quad (7)$$

One *E. coli* cell is assumed to be killed after reacting with α ROS. Thus, the oxidation reaction rate can be written as follows:

$$\frac{dC_t}{dt} = -k_0 C_{\text{ROS}}^{\alpha} C_t \quad (8)$$

where k_0 is the rate constant of the oxidation reaction and C_{ROS} is the concentration of ROS in the vicinity of *E. coli* cells resulting in bacterial inactivation. This equation is used based on the fundamental assumption that ROS are the dominant species in this process. The C_{ROS} can be strongly dependent on the discharge power and the feed gas used. The ROS resulting in the inactivation of *E. coli* cells can be both those dissolved in the water and those in the gas phase interacting with bacterial cells directly. During the discharge generated at a given V_P, the density of ROS in the gas phase is assumed to be independent of t. If C_{ROS} is mainly determined by the plasma density and remains constant at a given V_P, one can obtain the following equation by solving equation 8:

$$\log\left(\frac{C_t}{C_0}\right) = -k_0 C_{\text{ROS}}^{\alpha} t \log e = -k_0' t \quad (9)$$

where the value of the equation $k_0' = k_0 C_{\text{ROS}}^{\alpha} \log e$ is constant. Figure 3c shows a comparison between the $\log(C_t/C_0)$ values obtained within different treatment times and fitted theoretically by using equation 9. These fittings, resulting in a $k_0'(N_2)$ of 0.0039 s^{-1}, a k_0'(He) of 0.0098 s^{-1}, a k_0'(air) of 0.0022 s^{-1}, and a $k_0'(O_2)$ of 0.0033 s^{-1}, are consistent with the measured values ($R^2 > 0.95$ for all feed gases). This indicates that the plasma-generated oxidants in the gas phase can play a crucial role in killing the microorganisms. The inactivation efficiency is mainly determined by the density of oxidants generated inside microplasmas. Among these microplasma arrays, the O_2 microplasma array is most efficient at killing *E. coli* cells in water, which can be attributed to the relatively high density of oxidants generated inside O_2 microplasmas. Compared to H_2O_2 inactivation, the O_2 plasma can completely kill *E. coli* cells in water, since the $\log(C_t/C_0)$ value rapidly decreases with increasing treatment time. This can be attributed to the constant and high concentration of oxidants generated in O_2 microplasmas. Generally, O_2 and air plasmas are more effective at killing *E. coli* cells in water than N_2 and He plasmas. This also suggests that the oxygen-containing species generated inside O_2 or air microplasmas play a crucial role in activating *E. coli* cells in water.

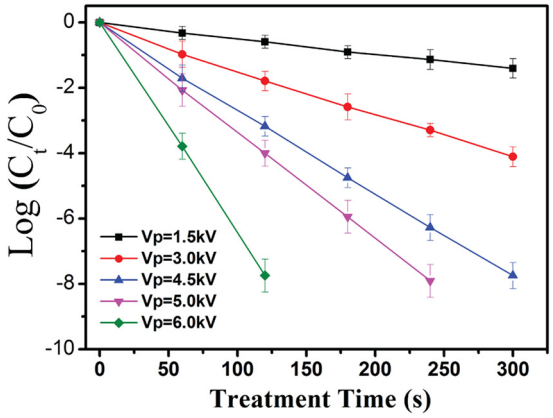

FIG 4 Comparison between $\log(C_t/C_0)$ values measured experimentally at different V_P values and fitted theoretically using equation 9. The data points and error bars represent, respectively, the averages and standard deviations from four independent measurements.

Figure 4 shows a comparison between the $\log(C_t/C_0)$ values measured experimentally at different V_P values and fitted theoretically by using equation 9. Clearly, the inactivation efficiency is strongly dependent on the V_P value. Increasing the V_P value leads to a significant increase in the inactivation efficiency. *E. coli* cells at a concentration of 10^6 CFU/ml were completely inactivated by the O_2 microplasma array generated at a V_P of 7.0 kV within a treatment time of 1.0 min. These theoretical fittings are consistent with the measured values. The $\log(C_t/C_0)$ values obtained at different V_P values linearly decrease with increasing treatment time. The slope of these straight lines is strongly dependent on the V_P value. These theoretical fittings lead to a k_0'(1.5 kV) of 0.0048 s^{-1}, a k_0'(3.0 kV) of 0.0013 s^{-1}, a k_0'(4.5 kV) of 0.0026 s^{-1}, a k_0'(5.0 kV) of 0.0032 s^{-1}, and a k_0'(6.0 kV) of 0.0065 s^{-1}, with correlation coefficients higher than 0.995. The value of the equation $k_0' = k_0 C_{\text{ROS}}^{\alpha} \log e$ obviously increases when the V_P is varied from 1.5 to 6.0 kV. These fittings predict that the ROS concentration of O_2 plasmas can be greatly improved at increasing V_P values.

OES spectra of microplasma jets. Figure 5 shows the typical OES spectra of N_2, He, air, and O_2 microplasma arrays generated at a V_P of 4.5 kV. The optical emissions from the second positive system of N_2 ($C^3\Pi \rightarrow B^3\Pi$) at 316, 337, 357, 380, and 405 nm (22, 23) and the first negative system of N_2^+ ($B^2\Sigma_u^+ \rightarrow X^2\Sigma_g^+$) at 391.4 nm (24) are observable for the N_2, He, air, and O_2 microplasma

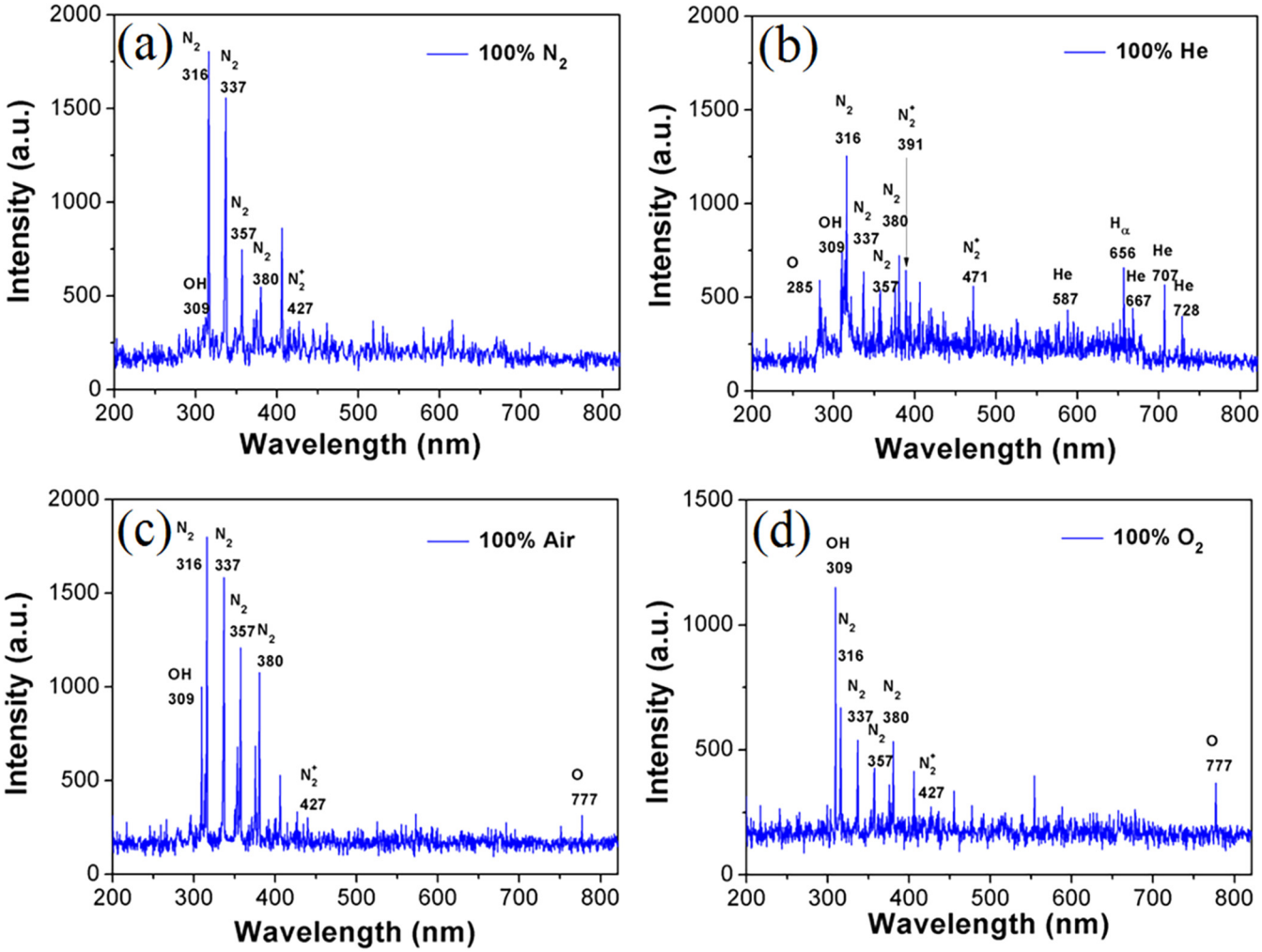

FIG 5 Typical OES spectra of the N_2, He, air, and O_2 microplasma arrays generated at a V_P of 4.5 kV. a.u., arbitrary units.

arrays. The N_2 ($B^3\Pi$ and $C^3\Pi$) and N_2^+ ($X^2\Sigma_g^+$) states are mainly formed by the electron impact excitation and ionization from the molecular ground state of N_2 ($X^1\Sigma_g^+$), respectively (25). In the He and O_2 microplasma arrays, the N_2 emissions could be from the residual N_2 molecules in the chamber. In the He microplasma array, the penning ionization process could be also responsible for the formation of N_2^+ in the gas phase (6). In the He microplasma array, He* atoms (metastable state) are mainly formed due to the collisions of energetic electrons with He atoms (26, 27). The OH emissions from the transition of $A^2\Sigma^+ \rightarrow X^2\Pi$ ($\Delta\nu = 0$) at 309 nm is also visible for the N_2, He, air, and O_2 microplasma arrays. The O_2 microplasma array shows the strongest OH emission, while the OH emission is weak in the N_2 microplasma array. Water vapor molecules may diffuse into the microplasmas, and OH radicals can be formed by electron impact dissociation ($H_2O + e^- \rightarrow H + OH + e^-$) (6). In the He microplasma array, OH radicals can be generated by the Penning process of excited He* and water vapor ($He^* + H_2O \rightarrow He + H + OH$) (6). The O emission at 777 nm, assigned to the transition of $2s^22p^33s$-$2s2sp^33p$ is visible for the air and O_2 microplasma arrays (26, 27). The energetic collisions of electrons with O_2 molecules ($O_2 + e^- \rightarrow 2O + e^-$) can be responsible for the formation of O radicals. The recombination process of O and H radicals ($O + H + M \rightarrow OH + M$) can contribute to the generation of OH radicals in the air and O_2 microplasma arrays.

pH value of the treated solution. The pH values of the solutions treated by using N_2, He, air, and O_2 microplasma arrays were measured as a function of the treatment time, as shown in Fig. 6. All the plasma treatments were performed at a V_P of 4.5 kV. The atmospheric-pressure air and N_2 microplasma arrays resulted in a slight decrease in the pH value. This could have been be due to the NO_x generated in the microplasmas. They react with water and produce nitric and nitrate acids (7, 16, 28). The pH values of the solutions treated by using O_2 and He microplasma arrays slightly increase with increasing treatment time. The energetic collisions of electrons with water vapor molecules can result in the formation of OH^- species in water (4, 7, 15, 29) and thus an increase in the pH value.

ROS concentration of the treated solution. In order to avoid the effect of holding time on the ROS concentration of the plasma-treated solutions exposed to the air, the ROS concentration was immediately measured by using the iodide oxidation-reduction method. ROS in the plasma-treated solutions or the hydrogen peroxide in the solution may rapidly react with manganese(II)

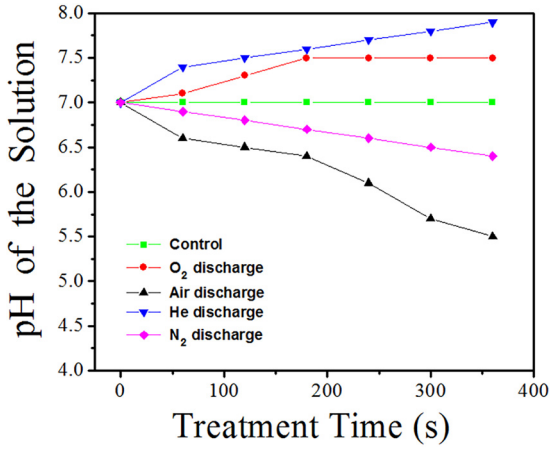

FIG 6 pH values of the solutions treated with N_2, He, air, and O_2 microplasma arrays as a function of the treatment time. All the plasma treatments were performed at a V_P of 4.5 kV.

ions when an excess of manganese(II) salt and iodide (I^-) and hydroxide (OH^-) ions are added to the solutions. Figure 7a shows the ROS concentrations in N_2, He, air, and O_2 plasma-treated solutions as a function of the plasma treatment time. The atmospheric-pressure microplasmas were generated at a V_P of 4.5 kV, corresponding to a discharge power of about 18 to 20 W. The ROS concentration increased when the treatment time varied from 0 to 420 s. The O_2 microplasma arrays showed the highest ROS concentration (~16 mg/liter) in the solution, while the ROS concentration in the N_2 microplasma-treated solution was relatively low (~1 mg/liter). The ROS concentration in the plasma-treated solutions is related to the efficiency of inactivation of *E. coli* cells in water. The higher the ROS concentration, the higher the inactivation efficiency, as shown in Fig. 3. The ROS concentration in the hydrogen peroxide solution exposed to the air was also measured as a function of the holding time. The measured ROS concentration in this solution was more than 10 g/liter. The concentration of ROS dissolved in the plasma-treated water was relatively low compared to that of the hydrogen peroxide solution.

Discharge power of microplasma arrays. The voltage-versus-charge plots or Lissajous figures of the N_2, He, air, and O_2 microplasma arrays were measured to calculate the discharge power. The discharge power showed little dependence on the feed gases used. However, the discharge power rapidly increased from 1.2 to 50 W with V_P values varying from 1.1 to 5.5 kV. The discharge energy consumption can be calculated from the average discharge power and the plasma treatment time required to completely kill *E. coli* cells in aqueous media. To obtain a 6-log-unit reduction of the *E. coli* cells in water, the discharge energy consumptions for atmospheric-pressure air and O_2 microplasma arrays were 0.38 to 0.66 kWh/m^3 and 0.33 to 0.52 kWh/m^3, respectively. The energy consumptions were much lower than those reported previously (30, 31). Bogomaz et al. (30) reported 5-log-unit reduction of *E. coli* cells with 1 kWh/m^3 by high-voltage pulsed discharge in water. Lee et al. (31) reported the disinfection of bacteria and viruses in a synthetic drinking water matrix with a pulsed arc discharge. *E. coli* inactivation ranged from approximately 0.8 log unit with 2.8 kWh/m^3 to 2.0 log units with 13.9 kWh/m^3. Plasma inactivation of *Photobacterium phosphoreum* and *Lactobacillus sakei* by surface dielectric barrier discharge resulted in a 3-log-unit or 4-log-unit reduction with 150 kWh/m^3 (32). An increase in the discharge power indicates an improvement in the density of the microplasmas generated in the aqueous media, and thus, an increase in the concentration of ROS reacting with microorganisms in water, as shown in Fig. 7b. As discussed previously (15), the average discharge power is significantly influenced by the flow rate, the spatial distribution of the microplasma units, the feed gases used, and the V_P. The average discharge power is proportional to the frequency of applied voltage, V_P, and the average discharge current. An increase in the high discharge power at an increasing V_P can be attributed to the strong pulsed discharges (15).

DISCUSSION

Plasma-induced species, such as radicals and charged particles (electrons and ions), have been assumed to play a role in the inactivation process by low-temperature plasmas (20, 33). It is thought that UV radiation from the atmospheric-pressure cold plasmas is insufficient to cause lethal damage to cells (2, 33, 34). In this study, the pH values of solutions are typically in the range of 5.6 to 7.8, depending on the feed gas used and the treatment time.

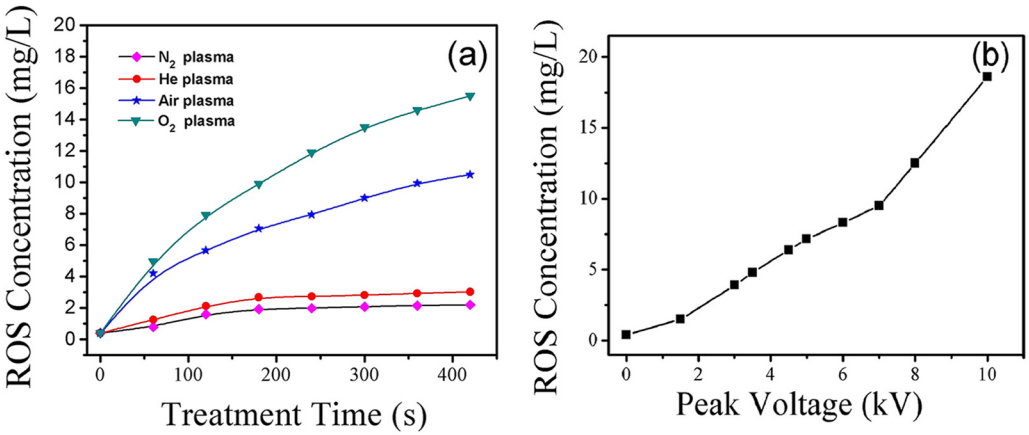

FIG 7 (a) ROS concentrations in N_2, He, air, and O_2 plasma-treated solutions as a function of plasma treatment time. The atmospheric-pressure microplasmas were generated at a V_P of 4.5 kV. (b) ROS concentrations in the O_2 plasma-treated solution as a function of V_P. The plasma treatment time remained constant at 100 s.

However, it has been proposed that the rate of inactivation of bacterial cells is not affected at all by the pH value of cultures when it is varied from 7 to 8 to 2.0 (4, 28). In addition, our measurements show that the temperature of the plasma-treated solution slowly increases from room temperature to about 40°C within a treatment time of 10 min, indicating that the slight increase in the water temperature does not cause an obvious effect on the survival efficiency of bacterial cells.

With this method, the microplasmas may be in direct contact with the bacterial cells in the aqueous solution, as described previously (6). In this study, plasma-generated ROS typically included the H_2O_2, HO_2, O_3, and nitrogen oxide (NO_x) molecules, HNO_x, and O and OH radicals in the gas phase. Among various plasma-activated neutrals, O and OH radicals and nitrogen-containing species (reactive nitrogen species [RNS]) have been assumed to play a reasonable role in the plasma inactivation of microorganisms (34–39). These species have a strong oxidative effect on the outer structures of bacterial cells. Since the O_2 microplasmas are more effective at inactivating *E. coli* cells than air microplasmas, the RNS generated in the air microplasmas are not proposed to play a crucial role in the inactivation process by this method. Reactive short-lived species, such as O and OH radicals, can be generated on site on the bacterial cells, since microplasmas are in direct contact with the cells suspended in the interface. These short-lived species can also dissolve in water and then react with *E. coli* cells suspended in the water. In fact, short-lived species dissolved in water, such as OH radicals, are considered to be the most important agents in the inactivation process (4). OH radicals can be easily formed even inside N_2 or He microplasmas when energetic electrons collide with water vapor. OES measurements have confirmed that OH radicals have been generated inside N_2, He, air, and O_2 microplasmas. In addition, a small amount of NaClO, with good efficacy in killing bacterial cells, may also be produced by plasma electrochemistry in 1% NaCl solution, but it does not affect our discussion and conclusions, since the sterilization effect of NaClO is caused by the NaClO-derived O-containing species, which can be regarded as plasma-induced ROS.

Our measurements show that among the N_2, He, air, and O_2 microplasma arrays, the O_2 microplasmas are most effective at killing *E. coli* cells suspended in water. This indicates that plasma-generated oxidants, such as ROS, can play a crucial role in the inactivation process. These ROS in the gas phase can immediately attack the *E. coli* cells suspended in the liquid-gas interface, or they may dissolve in the water and then react with *E. coli* cells suspended in the water. Increasing the discharge power leads to an improvement in the plasma density or ROS concentration and then an increase in the inactivation rate, as shown in Fig. 4. The variation of the efficiency of inactivation of *E. coli* cells in water with the treatment time is well explained by the chemical reaction rate model. In this model, the concentration of plasma-generated ROS plays the most important role in determining the inactivation rate of *E. coli* cells.

Compared with the atmospheric-pressure microplasma arrays generated at a V_P of 4.5 kV, the inactivation of *E. coli* cells by H_2O_2 solution is more effective at this initial stage. The H_2O_2 molecules may efficiently react with *E. coli* cells in water, acting as one ROS. However, the inactivation rate slowly decreases with increasing treatment time, which is due to the rapid reduction in the H_2O_2 concentration in water. The inactivation rates of *E. coli* cells in water with different treatment times can also be described by the chemical reaction rate model, as calculated previously. This model indicates that it can be difficult to completely kill *E. coli* cells in water by using H_2O_2 solution. However, the microplasma array may be used to efficiently kill *E. coli* cells in water, since the ROS density in the gas phase mainly depends on the discharge power and the feed gas used and does not significantly change with treatment time. When the ROS concentration remains unchanged, the $\log(C_t/C_0)$ value linearly decreases with the treatment time, as described in equation 9, resulting in the efficient inactivation of *E. coli* cells. The ozone molecules can be generated from the O_2 and air microplasma arrays. The ozone dissolved in water can decompose into highly reactive hydroxyl radicals (OH) (40–42). Initiation is the rate-limiting step that leads to formation of free radicals, superoxide radical ions, and hydroperoxide radicals: $O_3 + OH^- \rightarrow HO_2 + O_2^-$. Formation of these radicals leads to generation of the highly reactive radical OH, such as $H + HO_2 \rightarrow OH + OH$. In addition, ozone reacts slowly with saturated fatty acids and polysaccharides, while unsaturated fatty acids and sulfhydryl groups are readily oxidized by ozone (41, 42). These oxidization processes may lead to the inactivation of microorganisms and bacterial spores. The combination of ozone with appropriate initiators (for example, UV photons, H_2O_2, O, and OH radicals or charged species) can result in advanced oxidation processes that are potentially effective against the most resistant *E. coli* cells (41).

In this study, the plasma inactivation of *E. coli* cells suspended in water was performed by using atmospheric-pressure N_2, He, air, and O_2 microplasma arrays. Compared to the N_2 and He microplasma arrays, the air and O_2 microplasma arrays are more effective in inactivating *E. coli* cells in water. *E. coli* cells suspended in water are not completely inactivated by H_2O_2 solution, while the atmospheric-pressure arrays may be utilized to completely kill the *E. coli* cells in water. The chemical reaction rate models may be used to quantitatively describe the efficiencies of inactivation of *E. coli* cells by H_2O_2 solution and microplasma arrays. Analysis shows that the ROS play a crucial role in the inactivation process, and the inactivation rate of *E. coli* cells is strongly dependent on the concentration of plasma-activated oxidants.

ACKNOWLEDGMENTS

This work was supported by the Natural Science Foundation of Fujian Province, China (2014J01025), the National Natural Science Foundation of China (11275261), and the Fujian Provincial Key Laboratory for Plasma and Magnetic Resonance.

REFERENCES

1. **Laroussi M, Leipold F.** 2004. Evaluation of the roles of reactive species, heat, and UV radiation in the inactivation of bacterial cells by air plasmas at atmospheric pressure. Int J Mass Spectrom **233:**81–86. http://dx.doi.org/10.1016/j.ijms.2003.11.016.
2. **Lu XP, Ye T, Cao YG, Sun ZY, Xiong Q, Tang ZY, Xiong ZL, Hu J, Jiang ZH, Pan Y.** 2008. The roles of the various plasma agents in the inactivation of bacteria. J Appl Phys **104:**053309. http://dx.doi.org/10.1063/1.2977674.
3. **Locke B, Shih K.** 2011. Review of the methods to form hydrogen peroxide in electrical discharge plasma with liquid water. Plasma Sources Sci Technol **20:**034006. http://dx.doi.org/10.1088/0963-0252/20/3/034006.
4. **Sun P, Wu H, Bai N, Zhou H, Wang R, Feng H, Zhu W, Zhang J, Fang J.** 2012. Inactivation of Bacillus subtilis spores in water by a direct-current, cold atmospheric-pressure air plasma microjet. Plasma Process Polym **9:**157–164. http://dx.doi.org/10.1002/ppap.201100041.
5. **Sakiyama Y, Tomai T, Miyano M, Graves DB.** 2009. Disinfection of E. coli by nonthermal microplasma electrolysis in normal saline solution. Appl Phys Lett **94:**161501. http://dx.doi.org/10.1063/1.3122148.
6. **Zhang X, Liu D, Wang H, Liu L, Wang S, Yang S.** 2012. Highly effective

inactivation of Pseudomonas sp HB1 in water by atmospheric pressure microplasma jet array. Plasma Chem Plasma Process **32:**949–957. http://dx.doi.org/10.1007/s11090-012-9389-5.

7. **Du CM, Wang J, Zhang L, Li HX, Liu H, Xiong Y.** 2012. The application of a non-thermal plasma generated by gas-liquid gliding arc discharge in sterilization. J New Phys **14:**013010. http://dx.doi.org/10.1088/1367-2630/14/1/013010.
8. **Lu X, Naidis G, Laroussi M, Ostrikov K.** 2014. Guided ionization waves: theory and experiments. Phys Rep **540:**123–166. http://dx.doi.org/10.1016/j.physrep.2014.02.006.
9. **Tseng CC, Li CS.** 2006. Ozone for inactivation of aerosolized bacteriophages. Aerosol Sci Technol **40:**683–689. http://dx.doi.org/10.1080/02786820600796590.
10. **Thurston-Enriquez JA, Haas CN, Jacangelo J, Riley K, Gerba CP.** 2003. Inactivation of feline calicivirus and adenovirus type 40 by UV radiation. Appl Environ Microbiol **69:**577–582. http://dx.doi.org/10.1128/AEM.69.1.577-582.2003.
11. **Pottage T, Macken S, Giri K, Walker JT, Bennett AM.** 2012. Low temperature decontamination with hydrogen peroxide or chlorine dioxide for space applications. Appl Environ Microbiol **78:**4169–4174. http://dx.doi.org/10.1128/AEM.07948-11.
12. **Yao M, Mainelis G, An HR.** 2005. Inactivation of microorganisms using electrostatic fields. Environ Sci Technol **39:**3338–3344. http://dx.doi.org/10.1021/es048808x.
13. **Song Y, Liu DP, Lu QQ, Xia Y, Zhou RW, Yang DZ, Ji LF, Wang WC.** 2015. An atmospheric-pressure large-area diffuse surface dielectric barrier discharge used for disinfection application. IEEE Trans Plasma Sci **43:**821–827. http://dx.doi.org/10.1109/TPS.2015.2393952.
14. **Wu Y, Yao M.** 2010. Inactivation of bacteria and fungus aerosols using microwave irradiation. J Aerosol Sci **41:**682–693. http://dx.doi.org/10.1016/j.jaerosci.2010.04.004.
15. **Tang YZ, Lu XP, Laroussi M, Dobbs FC.** 2008. Sublethal and killing effects of atmospheric-pressure, nonthermal plasma on eukaryotic microalgae in aqueous media. Plasma Process Polym **5:**552. http://dx.doi.org/10.1002/ppap.200800014.
16. **Zhang X, Liu D, Song Y, Sun Y, Yang S.** 2013. Atmospheric-pressure air microplasma jets in aqueous media for the inactivation of Pseudomonas fluorescens cells. Phys Plasmas **20:**053501. http://dx.doi.org/10.1063/1.4803190.
17. **Geyter ND, Morent R, Gengembre L, Leys C, Payen E, Vlierberghe SV, Schacht E.** 2008. The inactivation of resistant Candida albicans in a sealed package by cold atmospheric pressure plasmas. Plasma Chem Plasma Process **28:**289–300. http://dx.doi.org/10.1007/s11090-008-9124-4.
18. **Numako C, Nakai I.** 1995. XAFS studies of some precipitation and coloration reaction used in analytical chemistry. Physica B Condens Matter **208-209:**387–388.
19. **Herbert D, Elsworth R, Telling RC.** 1956. The continuous culture of bacteria; a theoretical and experimental study. J Gen Microbiol **14:**601–622. http://dx.doi.org/10.1099/00221287-14-3-601.
20. **Laroussi M.** 2005. Low temperature plasma-based sterilization: overview and state-of-the-art. Plasma Process Polym **2:**391–400. http://dx.doi.org/10.1002/ppap.200400078.
21. **Lim JP, Uhm HS, Li SZ.** 2007. Influence of oxygen in atmospheric-pressure argon plasma jet on sterilization of Bacillus atrophaeous spores. J Appl Phys **14:**093504. http://dx.doi.org/10.1063/1.2773705.
22. **Khan FU, Rehman NU, Naseer S, Naveed MA, Qayyum A, Khattak NAD, Zakaullah M.** 2009. Diagnostic of 13.56 MHz RF sustained Ar–N_2 plasma by optical emission spectroscopy. Eur Phys J Appl Phys **45:**11002. http://dx.doi.org/10.1051/epjap:2008198.
23. **Sakamoto T, Matsuura H, Akatsuka H.** 2007. Spectroscopic study on the vibrational populations of N_2 $C^3\Pi$ and $B^3\Pi$ states in a microwave nitrogen discharge. J Appl Phys **101:**23307. http://dx.doi.org/10.1063/1.2426975.
24. **Sarani A, Nikiforov AY, Leys C.** 2010. Atmospheric pressure plasma jet in Ar and Ar/H_2O mixtures: optical emission spectroscopy and temperature measurements. Phys Plasmas **17:**063504. http://dx.doi.org/10.1063/1.3439685.
25. **Liu D, Niu J, Yu N.** 2011. Optical emission characteristics of medium- to high-pressure N_2 dielectric barrier discharge plasmas during surface modification of polymers. J Vac Sci Technol A **29:**061506. http://dx.doi.org/10.1116/1.3635372.
26. **Zhu W, Li Q, Zhu X, Pu Y.** 2009. Characteristics of atmospheric pressure plasma jets emerging into ambient air and helium. J Phys D Appl Phys **42:**202002. http://dx.doi.org/10.1088/0022-3727/42/20/202002.
27. **Golubovskii YB, Maiorov VA, Behnke J, Behnke JF.** 2003. Modelling of the homogeneous barrier discharge in helium at atmospheric pressure. J Phys D Appl Phys **36:**39. http://dx.doi.org/10.1088/0022-3727/36/1/306.
28. **Liu F, Sun P, Bai N, Tian Y, Zhou H, Wei S, Zhou Y, Zhang J, Zhu W, Becker K, Fang J.** 2010. Inactivation of bacteria in an aqueous environment by a direct-current, cold-atmospheric-pressure air plasma microjet. Plasma Process Polym **7:**231–236. http://dx.doi.org/10.1002/ppap.200900070.
29. **Tochikubo F, Uchida S, Watanabe T.** 2004. Study on decay characteristics of OH radical density in pulsed discharge in Ar/H_2O. Jpn J Appl Phys **43:**315–320. http://dx.doi.org/10.1143/JJAP.43.315.
30. **Bogomaz AA, Goryachev VL, Remennyi AS, Rutberg FG.** 1991. The effectiveness of a pulsed electrical discharge in decontaminating water. Sov Technol Phys Lett **17:**448.
31. **Lee LH, Arnold AJ, Santillan CA, Emelko MB, Dickson SE, Chang JS.** 2008. Bench-scale disinfection of bacteria and viruses with pulsed arc electrohydraulic discharge. Water Qual Res J Can **43:**77–84.
32. **Chiper AS, Chen W, Mejlholm O, Dalgaard P, Stamate E.** 2011. Atmospheric pressure plasma produced inside a closed package by a dielectric barrier discharge in Ar/CO_2 for bacterial inactivation of biological samples. Plasma Sources Sci Technol **20:**025008. http://dx.doi.org/10.1088/0963-0252/20/2/025008.
33. **Stoffels E, Sakiyama Y, Graves DB.** 2008. Cold atmospheric plasma: charged species and their interactions with cells and tissues. IEEE Trans Plasma Sci **36:**1441–1457. http://dx.doi.org/10.1109/TPS.2008.2001084.
34. **Laroussi M.** 2009. Low-temperature plasmas for medicine? IEEE Trans Plasma Sci **37:**714–725. http://dx.doi.org/10.1109/TPS.2009.2017267.
35. **Bai N, Sun P, Zhou H, Wu H, Wang R, Liu F, Zhu W, Lopez JL, Zhang J, Fang J.** 2011. Inactivation of Staphylococcus aureus in water by a cold, He/O_2 atmospheric pressure plasma microjet. Plasma Process Polym **8:**424–431. http://dx.doi.org/10.1002/ppap.201000078.
36. **Goree J, Liu B, Drake D.** 2006. Gas flow dependence for plasma-needle disinfection of S. mutans bacteria. J Phys D Appl Phys **39:**3479. http://dx.doi.org/10.1088/0022-3727/39/16/S05.
37. **Machala Z, Janda M, Hensel K.** 2007. Emission spectroscopy of atmospheric pressure plasmas for bio-medical and environmental applications. J Mol Spectrosc **243:**194–201. http://dx.doi.org/10.1016/j.jms.2007.03.001.
38. **Oehmigen K, Hähnel M, Brandenburg R, Wilke C, Weltmann KD, Woedtke TV.** 2010. The role of acidification for antimicrobial activity of atmospheric pressure plasma in liquids. Plasma Process Polym **7:**250–257. http://dx.doi.org/10.1002/ppap.200900077.
39. **Oehmigen K, Winter J, Hähnel M.** 2011. Estimation of possible mechanisms of Escherichia coli inactivation by plasma treated sodium chloride solution. Plasma Process Polym **8:**904–913. http://dx.doi.org/10.1002/ppap.201000099.
40. **Karaca H, Velioglu YS.** 2007. Ozone applications in fruit and vegetable processing. Food Rev Int **23:**91–106. http://dx.doi.org/10.1080/87559120600998221.
41. **Khadre MA, Yousef AE, Kim JG.** 2001. Microbiological aspects of ozone applications in food: a review. J Food Sci **66:**1242–1252. http://dx.doi.org/10.1111/j.1365-2621.2001.tb15196.x.
42. **Kim JG, Yousef AE, Dave S.** 1999. Application of ozone for enhancing the microbiological safety and quality of foods: a review. J Food Prot **62:**1071–1087.